Abstract: Refractive-index gradients induced in the atmospheric air by properly tailored laser and microwave fields are shown to enable a remote steering of laser beams. Heating-assisted modulation of the refractive index of the air by microwave radiation is shown to support small-angle laser-beam bending with bending angles on the order of 10^{-2}. Ionization of the atmospheric air by dyads of femto- and nanosecond laser pulses, on the other hand, can provide beam deflection angles in excess of $\pi/5$, offering an attractive strategy for radiation transfer, free-space communications, and laser-based standoff detection.

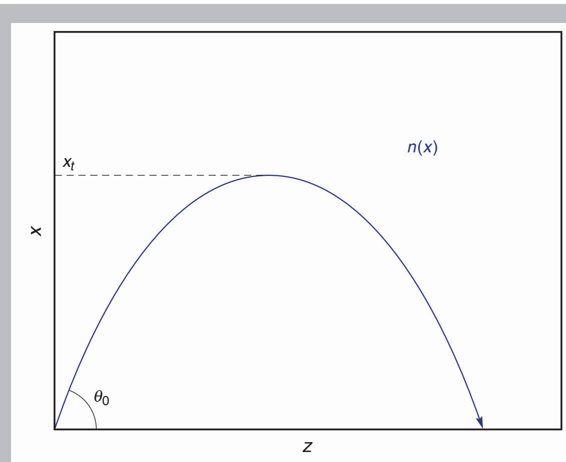

Trajectory of a laser beam against refractive-index gradient $n(x)$

Remote steering of laser beams by radar- and laser-induced refractive-index gradients in the atmosphere

A.M. Zheltikov, [1,2,*] *M.N. Shneider,* [3] *A.A. Voronin,* [2] *A.V. Sokolov,* [1] *and M.O. Scully* [1,3]

[1] Department of Physics and Astronomy, Texas A&M University, College Station, TX, USA
[2] Physics Department, International Laser Center, M.V. Lomonosov Moscow State University, Moscow 119992, Russia
[3] Department of Mechanical and Aerospace Engineering, Princeton University, Princeton, NJ, 08544-5263, USA

Received: 15 April 2011, Revised: 17 August 2011, Accepted: 20 August 2011
Published online: 2 November 2011

Key words: laser standoff detection; filamentation; beam steering

1. Introduction

Methods enabling a remote control of laser beams are in great demand for a broad class of laser technologies, ranging from long-distance free-space laser-based communications to optical standoff detection [1]. While on the laboratory scale, laser beams can be controlled and steered with a variety of efficient and compact tools [2], including electro-optic devices, liquid-crystal modulators, adaptive optics, and microphotonic components, the long-range transmission mode leaves much less freedom for the control over laser beams, limiting the utility of lasers for applications requiring a long-range transmission of signals and energy in situations where precise beam positioning or beam-trajectory bending is needed.

Recent studies have revealed attractive solutions for the remote control of radar beams using ionization induced in the atmosphere by ultrashort laser pulses [3–9]. Self-consistent plasma dynamics analysis shows [10] that a near- or mid-infrared laser pulse can tailor plasma decay in the wake of a filament, efficiently suppressing, through electron temperature increase, the attachment of electrons to neutral species and dissociative recombination; thus substantially increasing the plasma-guide lifetime and fa-

* Corresponding author: e-mail: zheltikov@physics.tamu.edu, zheltikov@phys.msu.ru

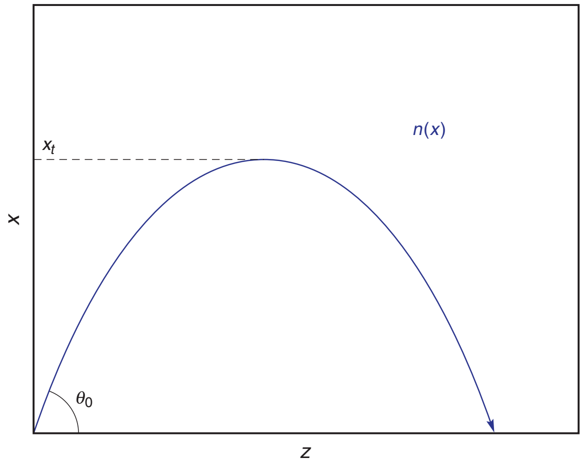

Figure 1 (online color at www.lphys.org) Trajectory of a laser beam against refractive-index gradient $n(x)$

cilitating long-distance transmission of microwaves. Here, we show that a combination of advanced laser systems, capable of supporting the filamentation mode of radiation transmission, with modern radar technologies or near- and mid-infrared laser sources offers much promise for the remote steering of laser beams and laser-induced filaments. In what follows, an eikonal analysis of beam trajectory will be combined with a detailed model of plasma dynamics in the atmosphere to examine the beam-steering abilities of laser- and radar-field-induced refractive-index gradients in the atmosphere.

2. Eikonal analysis

We consider the trajectory of a laser beam in a region with an arbitrary one-dimensional gradient of refractive index $n(x)$. The laser beam is assumed to enter this region at an angle θ_0 with respect to the z-axis, which is chosen to be perpendicular to the refractive-index gradient (Fig. 1). The eikonal equation for the laser-beam trajectory [11] then yields the equation for the beam trajectory [12]:

$$z(x) = \psi \int_0^x \frac{dx}{\sqrt{n^2(x) - \psi^2}}\,, \tag{1}$$

where

$$\psi = n(x)\cos\theta(x) = n(x)\frac{dz}{ds}$$

is the ray invariant, $\theta(x)$ is the angle between the beam and the z-axis for a current value of x, and s is the distance measured along the beam trajectory.

The turning point of the beam trajectory is defined by the equation

$$n(x_t) = \psi\,. \tag{2}$$

For a generic refractive-index profile

$$n^2(x) = n_0^2\left[1 - \left(\frac{x}{x_0}\right)^q\right], \quad 0 \le x \le x_{\max}\,, \tag{3}$$

where $x_{\max}$ is the boundary of the reflective index gradient, $q = 2$ corresponds to a parabolic profile and $q \to \infty$ recovers a step-index profile, the solution to Eq. (2) is given by

$$x_t = x_0\left(\frac{n_0^2 - \psi^2}{n_0^2}\right)^{\frac{1}{q}} = x_0\big(\sin\theta_0\big)^{\frac{2}{q}}\,. \tag{4}$$

The turning point exists only if

$$x_t \le x_{\max}\,. \tag{5}$$

The macroscopic approach used above is valid when the radiation wavelength is much longer than the distance between atoms. The scalar approximation is accurate enough as long as the refractive index varies on a spatial scale much larger than the radiation wavelength, failing for nanowaveguide-type structures [13–15].

3. Radar-induced refractive-index gradients

We first consider a refractive-index gradient induced in the atmosphere by a pair of overlapping radar beams in a standard atmosphere-probing geometry. Refraction gradient is then caused by a nonuniform heating of the atmospheric air with the maximum temperature and, hence, minimum molecular density achieved at the maximum of the interference pattern. The profile of the molecular density $N(x)$ will thus translate into the gradient of the refractive index:

$$n_r(x) = \sqrt{1 + \frac{\alpha N(x)}{\varepsilon_0}} \approx \tag{6}$$

$$\approx 1 + \frac{\alpha N(x)}{2\varepsilon_0} = n_a - \Delta n_r(x)\,,$$

$$n_a = 1 + \frac{\alpha N_0}{2\varepsilon_0}\,, \tag{7}$$

$$\Delta n_r(x) = \alpha\,\frac{N_0 - N(x)}{2\varepsilon_0}\,, \tag{8}$$

where α is the polarizability, ε_0 is the vacuum permittivity, and N_0 is the molecular density in the nonheated region.

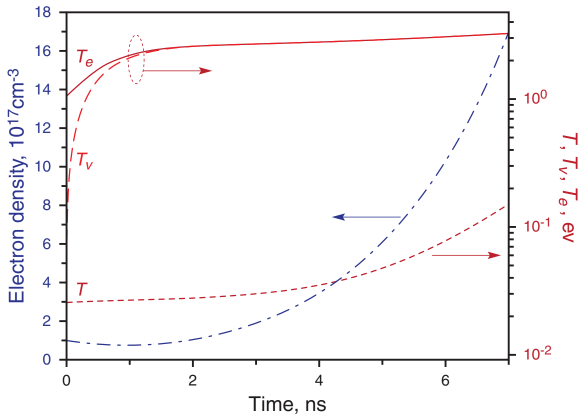

Figure 2 (online color at www.lphys.org) The on-axis electron density (dash-dotted curve) and the electron (solid line), vibrational (dashed line), and gas (dotted line) temperatures in the wake of a laser-induced filament in the presence of a laser pulse with a wavelength of 10.6 μm and intensity of 6.5×10^9 W/cm^2 as functions of the delay time with respect to filament generation by the femtosecond pulse

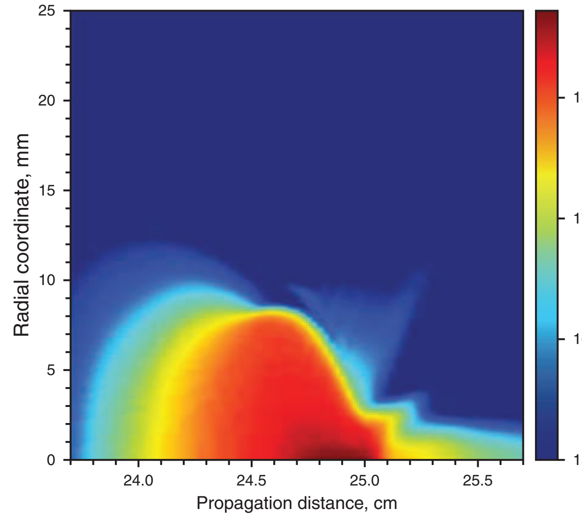

Figure 3 (online color at www.lphys.org) A two-dimensional map of electron density in a filament induced in the atmospheric air by a two-color laser field consisting of a 800-nm, 0.6-mJ, 25-fs pulse and a 400-nm, 0.09-mJ, 25-fs second harmonic focused with a 25-cm-focal-length lens)

At a constant pressure, Eq. (6) – Eq. (8) yield

$$\Delta n_r(x) = (n_a - 1)\left(\frac{290}{T[\mathrm{K}]} - 1\right), \quad (9)$$

where T[K] is the gas temperature in Kelvin degrees.

Setting the maximum value of the refractive index change equal to the high-temperature limit of Δn_r, $\Delta n_r(x_{\max}) = -\Delta n_{\max} = 1 - n_a$, we find for a parabolic refractive-index profile (Eq. (3) with $q = 2$) that

$$x_{\max} = x_0\sqrt{2\Delta n_{\max}}\,. \quad (10)$$

We now use Eq. (4), Eq. (5), and Eq. (10), to arrive at the following inequality limiting the maximum value of the θ_0 angle:

$$\sin\theta_0 \le \sin\theta_{\max} = \sqrt{2\Delta n_{\max}}\,. \quad (11)$$

With $\Delta n_{\max} \approx 3\times10^{-4}$, as in the case of atmospheric air, we find $\sin\theta_{\max} \approx \theta_{\max} \le 1.7\times10^{-2}$. A beam-deflection angle $\theta_d = 2\theta_{\max} \approx 3.4\times10^{-2}$ would correspond to beam bending over an obstacle as high as $h \approx 1.7$ m within a beam propagation path $l = 2h(\tan\theta_{\max})^{-1} \approx 200$ m.

4. Laser-induced refraction gradients

We now examine refractive-index gradients generated by femtosecond laser pulses in the wake of laser-induced filaments and tailored, as described in [10,16], by low-energy near- or mid-infrared laser pulses with longer, nanosecond-scale pulse widths. In this analysis, we employ a model of plasma dynamics based on a self-consistent integration of plasma-kinetic, Navier-Stokes, electron heat conduction, and electron-vibration energy transfer equations (see [10,17] for the details of this model). The model includes kinetic equations for the main species dominating atmospheric-air plasma chemistry in the wake of a laser-induced filament, such as oxygen, nitrogen, and ozone molecules (O_2, N_2, and O_3), molecular ions N_2^+, O_2^+, O_2^-, N_4^+, O_4^+, NO^+, oxygen and nitrogen atoms O and N, as well as atomic ions N^+, O^+, and O^-. Initial conditions for plasma parameters in the wake of a laser-induced filament are defined by solving the generalized nonlinear Schrödinger equation for an ultrashort laser pulse propagating through the atmosphere [18,19]. A typical two-dimensional map of the electron density induced by an ultrafast field waveform in the atmosphere is shown in Fig. 2. The key tendencies in the evolution of the plasma created in the wake of a laser filament and heated by a laser field with a central wavelength of 10.6 μm and intensity of 6.5×10^9 W/cm^2 is illustrated in Fig. 3 and Fig. 4. The mid-infrared field is seen to increase the electron, vibrational, and gas temperatures, as well as the electron density in the ionized gas (Fig. 3), giving rise to steeper gradients of the refractive index (Fig. 4).

Approximating the refractive index profile corresponding to a delay time $\tau_d = 6$ ns (relative to filament generation by the femtosecond pulse (Fig. 5a)) with a parabolic profile (Eq. (3) with $q = 2$), as shown by the dashed line in Fig. 5a, and using Eq. (10), we find that Eq. (11) holds true

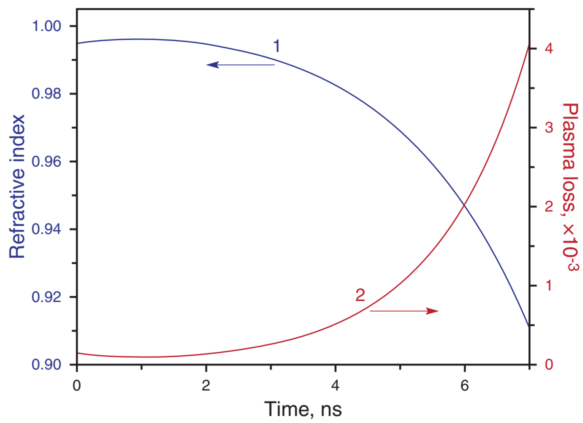

Figure 4 (online color at www.lphys.org) The refractive index (1) and plasma loss (2) of the atmospheric air in the presence of a laser pulse with a wavelength of 10.6 μm and intensity of 6.5×10^9 W/cm^2 in the wake of a laser-induced filament as a function of the delay time with respect to filament generation by the femtosecond pulse (instantaneous on this time scale)

for $\theta_{\max}$, with $\Delta n_{\max}$ now understood as the maximum change in the refractive index induced by ionization on the axis of the plasma column. For the chosen delay time of 6 ns, $\Delta n_{\max} \approx 0.05$, and the maximum beam-deflection angle is $\theta_d = 2\theta_{max} \approx 38°$. With such a beam-deflection technique, $M = 5$ reflections from properly arranged ionized gas layers would be sufficient for the reversal of the beam propagation direction. Reflection will typically take place within an area with a transverse size of 0.1 mm and a longitudinal size of 1 mm.

Plasma-induced attenuation of laser intensity over the entire beam path inside the ionized region is calculated as

$$\mu = \exp\left\{ \frac{4\pi}{\lambda} \int_0^{x_t} \frac{\kappa(x)}{\sqrt{n^2(x) - \psi^2}} dx \right\}$$

with the time-dependent plasma loss profile

$$\kappa(x,t) = \frac{1}{\sqrt{2}} \sqrt{-\varepsilon(x,t) + \sqrt{\varepsilon^2(x,t) + \left[\frac{4\pi\sigma(x,t)}{\omega}\right]^2}},$$

where

$$\varepsilon(x,t) = 1 - \frac{\omega_p^2(x,t)}{\omega^2 + \nu^2(x,t)},$$

e is the electron charge, $n_e(x,t)$ is the time-dependent electron density, ω is the radiation frequency,

$$\omega_p(x,t) = \sqrt{\frac{4\pi e^2 n_e(x,t)}{m}}$$

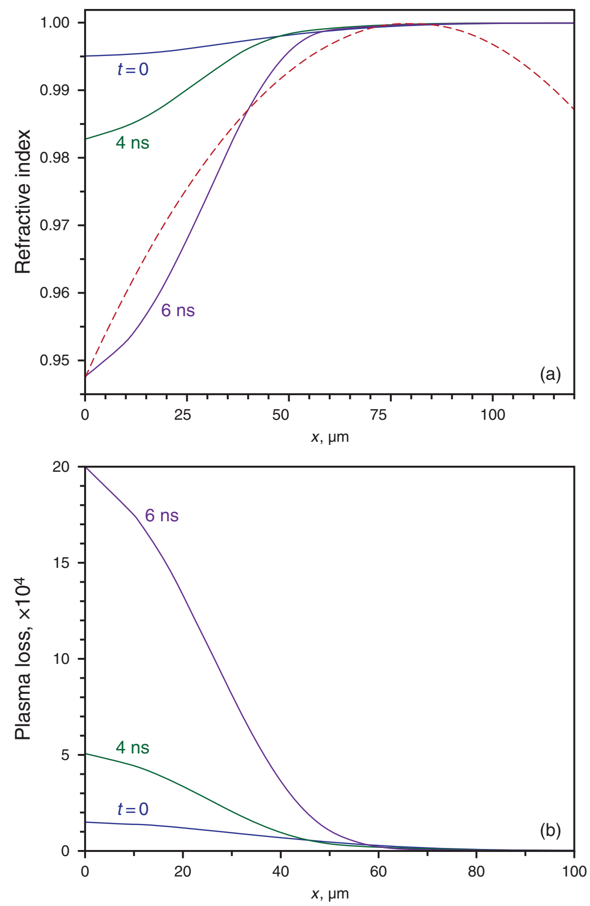

Figure 5 (online color at www.lphys.org) Refractive-index (a) and plasma loss (b) gradients induced in the atmospheric air in the presence of a laser pulse with a wavelength of 10.6 μm and intensity of 6.5×10^9 W/cm^2 for different delay times (0, 4, and 6 ns, as indicated next to the curves) relative to filament generation by the femtosecond pulse. The dashed line shows a parabolic fit of the refractive-index profile using Eq. (7) with $q = 2$

is the plasma frequency, m is the electron mass, and $\nu(t)$ is the effective collision frequency, defined as the imaginary part of the complex plasma refractive index. Kinetics of the plasma loss κ induced in the atmospheric air by a heating laser pulse with a wavelength of 10.6 μm and intensity of 6.5×10^9 W/cm^2 in the wake of a laser-induced filament calculated as a function of the delay time with respect to filament generation by the femtosecond pulse is shown by line 2 in Fig. 4. Computation of the integral for μ with the plasma loss profile $\kappa(x,t)$ found with the use of our plasma-dynamics model (shown in Fig. 5b for different delay time τ_d) yields an attenuation factor $\mu \approx 1.8$ for $\lambda = 10.6$ μm and $\tau_d = 6$ ns. The loss due to the scattering of a laser beam by fluctuations of the refractive index of the ionized air under these conditions did not exceed 1%. We note the connection between the present work and the recent experiment [20] in a coherently driven ultradispersive medium showing a strong "prisming", or deflection of a light beam. There, a deflection on the order of 0.1 rad was attainable, in essential agreement with the present paper. Other pertinent work includes remotely pumped lasing in the atmosphere [21,22] and applications of backward lasing in the atmosphere for standoff detection using coherent Raman scattering [23].

5. Conclusion

We have shown here that refractive-index gradients induced in the atmospheric air by properly tailored laser and microwave fields are shown to enable a remote steering of laser beams. Heating-assisted modulation of the refractive index of the air by microwave radiation is shown to support small-angle laser-beam bending with bending angles on the order of 10^{-2}. Ionization of the atmospheric air by dyads of femto- and nanosecond laser pulses, on the other hand, can provide beam deflection angles in excess of $\pi/5$, offering an attractive strategy for radiation transfer, free-space communications, and laser-based standoff detection.

Acknowledgements The research leading to these results has received funding from the European Union Seventh Framework Program (FP7/2007-2013 and FP7/2007-2011) under grant agreement No. 244068. This work has been also supported in part by the Office of Naval Research and the Robert A. Welch Foundation (projects A-1261 and A-1547). An access to the Lomonosov supercomputer granted by Moscow State University is gratefully acknowledged.

References

[1] V. Kocharovsky, S. Cameron, K. Lehmann, R. Lucht, R. Miles, Y. Rostovtsev, W. Warren, G.R. Welch, and M.O. Scully, Proc. Natl. Acad. Sci. **102**, 7806 (2005).
[2] A. Yariv and P. Yeh, Optical Waves in Crystals. Propagation and Control of Laser Radiation (Wiley, New York, 1984).
[3] M.N. Shneider and R.B. Miles, J. Appl. Phys. **98**, 033301 (2005).
[4] A.M. Zheltikov, M.N. Shneider, and R.B. Miles, Appl. Phys. B **83**, 149 (2006).
[5] M.N. Shneider, Z.L. Zhang, and R.B. Miles, J. Appl. Phys. **102**, 123103 (2007).
[6] R. Miles, Z.L. Zhang, S. Zaidi, and M. Shneider, AIAA J. **45**, 513 (2007).
[7] R.R. Musin, M.N. Shneider, A.M. Zheltikov, and R.B. Miles, Appl. Opt. **46**, 5593 (2007).
[8] M. Châteauneuf, S. Payeur, J. Dubois, and J.-C. Kieffer, Appl. Phys. Lett. **92**, 091104 (2008).
[9] V.D. Zvorykin, A.O. Levchenko, N.N. Ustinovskii, and I.V. Smetanin, JETP Lett. **91**, 226 (2010).
[10] M.N. Shneider, A.M. Zheltikov, and R.B. Miles, J. Appl. Phys. **108**, 033113 (2010).
[11] M. Born and E. Wolf, Principles of Optics. Electromagnetic Theory of Propagation, Interference and Diffraction of Light, 7th ed. (Cambridge University Press, Cambridge, 1999).
[12] A.W. Snyder and J.D. Love, Optical Waveguide Theory (Chapman and Hall, Ltd., London – New York, 1983).
[13] D.A. Sidorov-Biryukov, K.A. Kudinov, A.A. Podshivalov, and A.M. Zheltikov, Laser Phys. Lett. **7**, 355 (2010).
[14] Y.-J. Song, M.-L. Hu, C.-L. Gu, L. Chai, C.-Y. Wang, and A.M. Zheltikov, Laser Phys. Lett. **7**, 230 (2010).
[15] I.V. Fedotov, A.A. Lanin, V.I. Sokolov, A.B. Fedotov, A.S. Akhmanov, V.Ya. Panchenko, and A.M. Zheltikov, Laser Phys. Lett. **7**, 657 (2010).
[16] Z. Henis, G. Milikh, K. Papadopoulos, and A. Zigler, J. Appl. Phys. **103**, 103111 (2008).
[17] M.N. Shneider, A.M. Zheltikov, and R.B. Miles, Phys. Plasmas **18**, 063509 (2011).
[18] A. Couairon and A. Mysyrowicz, Phys. Rep. **441**, 47 (2007).
[19] V.P. Kandidov, S.A. Shlenov, and O.G. Kosareva, Quantum Electron. **39**, 205 (2009).
[20] V.A. Sautenkov, H.B. Li, Y.V. Rostovtsev, and M.O. Scully, Phys. Rev. A **81**, 063824 (2010).
[21] A. Dogariu, J.B. Michael, M.O. Scully, and R.B. Miles, Science **331**, 442 (2011).
[22] A. Traverso, R. Sanchez-Gonzalez, M.P. Grubb, D.V. Voronine, K. Wang, L.Q. Yuan, A. Zheltikov, A. Dogariu, J. Michael, R.B. Miles, V. Sautenkov, A. Sokolov, S.W. North, and M.O. Scully, in: Book of Abstracts of the 41st Winter Colloquium on the Physics of Quantum Electronics, Snowbird, UT, USA, January 2–6, 2011 (PQE-2011), p. 263.
[23] L. Yuan, A.A. Lanin, P.K. Jha, A.J. Traverso, D.V. Voronine, K.E. Dorfman, A.B. Fedotov, G.R. Welch, A.V. Sokolov, A.M. Zheltikov, and M.O. Scully, Laser Phys. Lett. **8**, 736 (2011).